Current Research in Toxicology 1 (2020) 111–115

Contents lists available at ScienceDirect

Current Research in Toxicology

journal homepage: www.elsevier.com/locate/crtox

Luminespib counteracts the Kifunensine-induced lung endothelial barrier dysfunction

Khadeja-Tul Kubra, Mohammad A. Uddin, Mohammad S. Akhter, Nektarios Barabutis *

School of Basic Pharmaceutical and Toxicological Sciences, College of Pharmacy, University of Louisiana Monroe, Monroe, LA 71201, United States of America

ARTICLE INFO

Article history:
Received 24 August 2020
Received in revised form 15 September 2020
Accepted 21 September 2020

Keywords:
P53
Endothelium
Inflammation
Acute lung injury

ABSTRACT

Unfolded protein response (UPR) suppression by Kifunensine has been associated with lung hyperpermeability, the hallmark of Acute Respiratory Distress Syndrome. The present study investigates the effects of the heat shock protein 90 inhibitor Luminespib (AUY-922) towards the Kifunensine-triggered lung endothelial dysfunction. Our results indicate that the UPR inducer Luminespib counteracts the effects of Kifunensine in both human and bovine lung endothelial cells. Hence, we suggest that mild UPR induction may serve as a promising therapeutic strategy against potentially lethal respiratory disorders, including the ARDS related to COVID-19.

1. Introduction

The pulmonary vasculature forms a continuous monolayer of endothelial cells to act as a semi-permeable barrier to control the extravasation of blood fluid, electrolytes, proteins and leukocytes. Dysregulation of lung endothelial barrier function due to lung inflammation has been associated with hyperpermeability responses across the endothelial and epithelial barriers. Such events contribute to the development of acute lung injury (ALI) and acute respiratory distress syndrome (ARDS) (Good et al., 2018). Patients hospitalized due to severe ARDS are subjected to mechanical ventilation and the risk of death in such instances may rise up to 45%, especially in the elderly. Hence, the development of novel therapeutic strategies towards the enhancement of lung endothelial barrier may deliver novel therapeutic possibilities in ARDS, including the ARDS related to COVID-19 (Torres Acosta and Singer, 2020).

Heat shock protein 90 (Hsp90) is a highly abundant molecular chaperone, essential for many fundamental processes including cell signaling, proliferation, differentiation, and survival (Scieglinska et al., 2019; Barabutis, 2020a). It is required for the folding, stability, and maturation of various client proteins (e.g. kinases, transcription factors, steroid hormone receptors) which are involved and propel inflammatory processes. Moreover, inflammatory stimuli (e.g. LPS) have been shown to activate (phosphorylate) Hsp90 (Abbasi et al., 2020; Barabutis et al., 2013). On the other hand, Hsp90 inhibition by the corresponding compounds (Hsp90 inhibitors) delivers an exciting possibility towards inflammatory conditions, including cancers (Barabutis and Siejka, 2020). An emerging body of evidence indicates that Hsp90 inhibitors oppose cancer and inflammation (Barabutis et al., 2018a). In experimental models of ALI/ARDS, Hsp90 inhibition counteracts lung endothelial hyperpermeability by remodeling the actin cytoskeleton (Barabutis et al., 2018b; Barabutis, 2020b).

Those effects involve the endothelial defender and tumor suppressor P53, which senses threats to devise cellular responses (Muller et al., 2004; Kubra et al., 2020a). The mild induction of this 53 kDa protein exerts anti-inflammatory effects in the lungs, linked to the decrease of the reactive oxygen species production (Akhter et al., 2020a). We have shown that Hsp90 inhibitors suppress the LPS-induced P53 phosphorylation, protecting this transcription factor against degradation (Barabutis et al., 2019). Moreover, those anti-cancer compounds stabilize P53 by reducing both in vivo and in vitro MDM2 and MDM4 (P53 negative regulators) (Barabutis et al., 2015).

The unfolded protein response (UPR) affects P53 in a positive manner (Akhter et al., 2019). This is an endoplasmic reticulum (ER)-based mechanism; which organizes cellular repairing processes (Barabutis, 2019a). The protein kinase RNA-like ER kinase (PERK), the activating transcription factor 6 (ATF6), and the inositol-requiring enzyme-1α (IRE1α) are the major elements of that mechanism, which bind to the immunoglobulin heavy chain binding protein (BiP) (Barabutis, 2019b). Increased ER stress disassociates BiP from the previously mentioned UPR components, leading to their activation (Kubra et al., 2020b). Interestingly, the Hsp90 inhibitors, 17-AAG, 17- DMAG, and AUY-922 induce UPR in both bovine and human lung endothelial cells, as well as in lungs from mice (Uddin et al., 2020a; Kubra et al., 2020c). Moreover, the α-mannosidases inhibitor and UPR

* Corresponding author at: School of Basic Pharmaceutical and Toxicological Sciences, College of Pharmacy, University of Louisiana Monroe, 1800 Bienville Drive, Monroe, LA 71201, United States of America.
E-mail address: barabutis@ulm.edu. (N. Barabutis).

http://dx.doi.org/10.1016/j.crtox.2020.09.003

suppressor Kifunensine (KIF) disrupted the lung endothelial barrier integrity, as reflected in measurements of transendothelial resistance (TEER) and key mediators of the vascular permeability (Akhter et al., 2020b). In the current study, we employed the UPR suppressor (KIF) and the Hsp90 inhibitor (Luminespib) to investigate whether Hsp90 inhibition supports the endothelium against the Kifunensine-induced lung endothelial barrier dysfunction.

2. Materials and methods

2.1. Reagents

Kifunensine (IC15995201), Luminespib (AUY-922) (101756-820), anti-mouse IgG HRP linked whole antibody from sheep (95017-554), anti-rabbit IgG HRP linked whole antibody from donkey (95017-556) and nitrocellulose membranes (10063-173), radioimmunoprecipitation assay (RIPA) buffer (AAJ63306-AP), as well as 3-(4,5-Dimethylthiazol-2-yl)-2,5-diphenyltetrazolium bromide (MTT) (BT142015-5G) were obtained from VWR (Radnor, PA). Phospho-cofilin (3313S), Cofilin (3318S), phospho-myosin light chain 2 (3674S), myosin light chain 2 (3672S) and P53 (9282S) antibodies were purchased from Cell Signaling Technology (Danvers, MA). The β-actin antibody (A5441) was purchased from Sigma-Aldrich (St Louis, MO).

2.2. Cell culture

Bovine pulmonary artery endothelial cells (BPAEC) (PB30205) were purchased from Genlantis (San Diego, CA) as well as human lung microvascular endothelial cells (HuLEC–5a) (CRL–3244) from American Type Culture Collection (Manassas, VA). Bovine cells were cultured in DMEM medium (VWRL0101-0500) supplemented with 10% fetal bovine serum (89510-186), and the human cells in PromoCell endothelial cell growth medium MV (10172-280). Those media were supplemented with 1 × penicillin/streptomycin (97063-708) and cells were maintained at 37 °C, in a humidified atmosphere of 5% CO_2/95% air. All reagents were purchased from VWR (Radnor, PA).

2.3. Measurement of cell viability

BPAECs were seeded in 96-well culture plates (10,000 cells/well) in complete growth media and were treated with KIF (0.01–200 μM) and AUY-922 (0.01–200 μM). After 24 h, media was replaced with serum-free media containing 0.5 mg/ml 3-(4, 5-Dimethylthiazol-2-yl)-2,5-diphenyltetrazolium bromide (MTT). After 3 h of incubation, DMSO (100 μl/well) was added to dissolve MTT crystals and 15 min later absorbance was measured at 570 nm on Synergy H1 Hybrid Multi-Mode Reader from Biotek (Winooski, VT).

2.4. Measurement of endothelial barrier function

The barrier function of endothelial cell monolayers grown on electrode arrays (8W10E+) was estimated by electric cell-substrate impedance sensing (ECIS), utilizing ECIS model ZΘ (Applied Biophysics, Troy, NY, USA). All experiments were conducted on wells which had reached a steady-state resistance of at least 800 Ω (Uddin et al., 2019a).

2.5. Western blot analysis

RIPA buffer and the EZBlock™ protease inhibitor cocktail were used to isolate the proteins from the cells. Protein-matched samples were separated according to their molecular weight by electrophoresis onto 12% sodium dodecyl sulfate Tris-HCl gels. Then, we employed a wet transfer technique to transfer the proteins onto the nitrocellulose membranes. The membranes were exposed for at least 60 min at room temperature in a solution of 5% non-fat dry milk. After incubating, the blots were exposed overnight (4 °C) to appropriate primary antibodies (1:1000). The following day, the membranes were incubated with the corresponding secondary antibodies (1:2000) to develop the signal for immunoreactive proteins. Protein signal was detected using chemiluminescent substrate (Thermo Scientific). All the images were captured using ChemiDoc™ Touch Imaging System from Bio-Rad (Hercules, CA). The β-actin was used as a loading control unless indicated otherwise. All reagents were purchased from VWR (Radnor, PA).

2.6. Densitometry and statistical analysis

Image J software (National Institute of Health) was used to perform densitometry of immunoblots. All data are expressed as mean values ± SEM (standard error of mean). Student's *t*-test was performed to determine statistically significant differences among groups. A value of $P < 0.05$ was considered significant. GraphPad Prism (version 5.01) was used to analyze the data. The letter n represents the number of experimental repeats.

3. Results

3.1. Hsp90 inhibitor luminespib (AUY-922) suppressed the KIF-induced activation of cofilin in BPAEC

Bovine lung cells were grown in six well plates. Confluent cells were pretreated with either vehicle (0.1% DMSO), or 5 μM of KIF for 24 h. After 16 h of post-treatment with AUY-922, we investigated the effects of those treatments in the phosphorylation of Cofilin (pCofilin). As shown in Fig. 1A, UPR suppression decreased the phosphorylated cofilin and luminespib opposed that effect.

3.2. Luminespib suppressed the KIF-induced phosphorylation of MLC2 in BPAEC

BPAEC were pretreated with either vehicle (0.1% DMSO) or the UPR suppressor KIF (5 μM) for 24 h, followed by treatment with either vehicle (0.1% DMSO) or luminespib (2 μM). After 16 h of AUY-922 exposure, we investigated the effects of UPR suppression in the phosphorylation of myosin light chain 2. Our results suggest that KIF significantly induces the phosphorylated MLC2 (pMLC2) level and the Hsp90 inhibitor luminespib downregulated that MLC2 phosphorylation in KIF-treated cells (Fig. 1B).

3.3. Luminespib suppressed the KIF-induced phosphorylation of MLC2 in HuLEC-5a

Human lung endothelial cells were exposed to either vehicle (0.1% DMSO) or KIF (5 μM). After 24 h of KIF exposure, the cells were treated with either vehicle (0.1% DMSO) or luminespib (2 μM) for 16 h. Western blot analysis was performed on cell lysates to measure protein levels. The densitometry analysis of the immunoblots revealed that KIF significantly induces the phosphorylation of MLC2 (pMLC2), while AUY-922 remarkably reduces the activation of MLC2 in KIF-treated human lung endothelial cells (Fig. 1C).

3.4. Luminespib protects against the KIF-induced endothelial barrier hyperpermeability in BPAEC

We employed the electric cell-substrate impedance sensing (ECIS) model to evaluate the lung endothelial barrier function. BPAEC were seeded onto the gold electrode arrays and left to reach steady transendothelial values, an indicator of the monolayer formation. The cells were treated with either vehicle (0.1% DMSO) or KIF (25 μM) for 18 h prior to treatment with either vehicle (0.1% DMSO) or AUY-922 (5 μM). Treatment with KIF to the lung cells exerted decreased TEER values (increased permeability). Luminespib (5 μM) post-treatment prevented the Kifunensine-triggered hyperpermeability, as reflected in the increased TEER values (Fig. 1D).

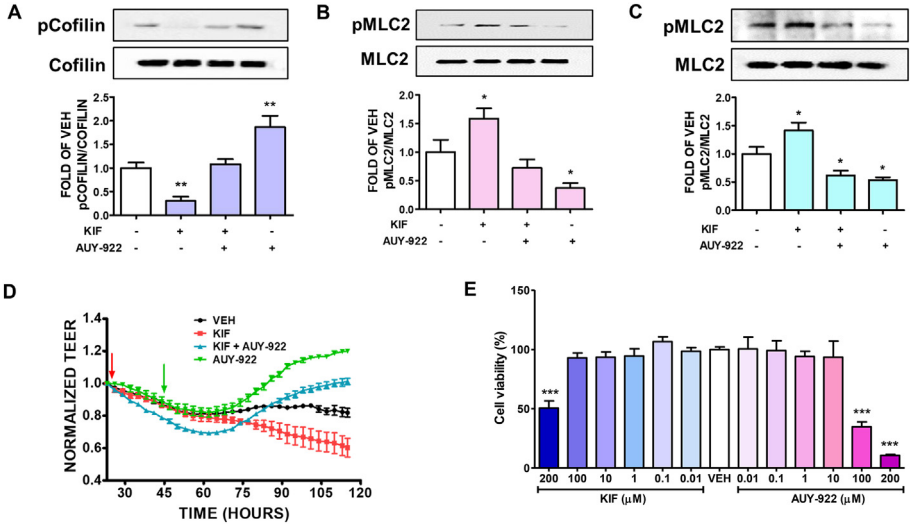

Fig. 1. Effects of KIF and AUY-922 on lung endothelial cells. Western Blot analysis of (A) phosphorylated Cofilin (pCofilin) and Cofilin (B) phosphorylated MLC2 (pMLC2) and MLC2 after 24 h treatment of BPAEC with either KIF (5 μM) or vehicle (0.1% DMSO) and post-treatment with AUY-922 (2 μM) or vehicle (0.1% DMSO) for 16 h. The blots shown are representative of 4 independent experiments. The signal intensity of the bands was analyzed by densitometry. Protein levels of pCofilin and pMLC2 were normalized to Cofilin and MLC2 respectively. $^{*}P < 0.05$, $^{**}P < 0.01$ vs vehicle. Means ± SEM. Western Blot analysis of (C) phosphorylated MLC2 (pMLC2) and MLC2 after 24 h treatment of HuLEC with either KIF (5 μM) or vehicle (0.1% DMSO); and post-treatment with AUY-922 (2 μM) or vehicle (0.1% DMSO) for 16 h. The blots shown are representative of 3 independent experiments. The signal intensity of the pMLC2 was analyzed by densitometry. Protein levels of pMLC2 were normalized to MLC2. *P < 0.05 vs vehicle. Means ± SEM. (D) Confluent monolayers of BPAEC were pre-treated with either vehicle (0.1% DMSO) or KIF (25 μM) (red arrow) for 18 h, followed by treatment with either vehicle (0.1% DMSO) or 5 μM of AUY-922 (green arrow). A gradual increase in endothelial permeability (reduced TEER) was observed in KIF treated cells (red line). AUY-922 significantly reduced the endothelial permeability (increased TEER) in both KIF-pretreated (blue line) and vehicle-treated cells (green line). (E) Cells were incubated with either VEH (0.1% DMSO) or KIF (0.01, 0.1, 1, 10, 100, 200 μM) or AUY-922 (0.01, 0.1, 1, 10, 100, 200 μM) for 24 h. Cellular viability was evaluated by employing the MTT assay. $^{***}P < 0.001$ vs VEH, $n = 3$. Means ± SEM.

3.5. Effects of KIF and luminespib (AUY-922) in cellular viability

BPAECs were seeded on 96-well plate (10,000 cells in each well) and treated with either vehicle (0.1% DMSO) or KIF (0.01–200 μM) or AUY-922 (0.01–200 μM) for 24 h. Our results suggest that moderate concentrations of KIF (0.01–100 μM) and luminespib (0.01–10 μM) do not exhibit toxicity to bovine lung endothelial cells (Fig. 1E). However, cells exposed to higher concentrations of KIF (200 μM) and AUY-922 (100 and 200 μM) demonstrated significant reduction in their cellular viability.

3.6. Luminespib (AUY-922) inhibits the KIF-induced suppression of P53 in BPAEC

To investigate the supportive effects of AUY-922 against KIF-induced hyperpermeability in BPAEC, we pretreated BPAEC with either vehicle (0.1% DMSO) or KIF (5 μM) for 24 h. The cells were post-treated with either vehicle (0.1% DMSO) or AUY-922 (2 μM). After 16 h of AUY-922 post-treatment, western blot analysis was performed to detect P53 expression levels. KIF significantly reduced P53 abundance, while luminespib inhibited that effect. Moreover, this Hsp90 inhibitor significantly induced P53 levels (Fig. 2A).

3.7. Luminespib (AUY-922) reduces the KIF-triggered induction of MDM2 in BPAEC

BPAEC were exposed to either vehicle (0.1% DMSO) or KIF (5 μM) for 24 h. After that treatment, the cells were treated with either vehicle (0.1% DMSO) or 2 μM of luminespib for 16 h. The KIF-treated cells exhibited higher levels of MDM2, while AUY-922 reversed that effect (Fig. 2B).

3.8. Luminespib (AUY-922) inhibits KIF-induced suppression of P53 in HuLEC-5a

Human lung endothelial cells were pretreated with either vehicle (0.1% DMSO) or KIF (5 μM) for 24 h, followed by treatment with either vehicle (0.1% DMSO) or 2 μM of AUY-922. After 16 h of AUY-922 exposure, we performed densitometric analysis in the immunoblots. Fig. 2C shows that KIF significantly reduces P53 expression, while luminespib prevents that effect in KIF-treated cells.

3.9. Luminespib (AUY-922) prevents KIF-mediated induction of MDM2 in HuLEC-5a

HuLEC-5a were pretreated with either vehicle (0.1% DMSO) or KIF (5 μM). After 24 h of KIF exposure, the cells were treated with either vehicle (0.1% DMSO) or luminespib (2 μM) for 16 h. KIF promoted the induction of the P53 inhibitor MDM2, and AUY-922 significantly counteracted that effect (Fig. 2D).

4. Discussion

Investigating the molecular mechanisms involved in the mediation of the anti-inflammatory activities of the Hsp90 inhibitors in the vasculature expands our knowledge on the regulation of the lung endothelial barrier function. C-terminal domain-based Hsp90 inhibitors protect against the bacteria-induced endothelial barrier dysfunction (Joshi et al., 2014; Solopov et al., 2020). In the current work, we evaluated the effects of UPR manipulation towards the lung endothelial permeability. We employed the Hsp90 inhibitor AUY-922 (UPR inducer), as well as the UPR suppressor Kifunensine (a selective inhibitor of class 1 α-mannosidases) to evaluate their effects towards lung endothelial permeability. Luminespib represents an advanced stage in the development of Hsp90 inhibitors. It has been associated with minimum side effects, and has advanced to Phase II of clinical trials to fight cancer (Felip et al., 2018).

In our study, Luminespib opposed the KIF-induced phosphorylation of myosin light chain (MLC2) in both bovine and human lung endothelial cells (Fig. 1B, C). Myosin light chain kinases (MLCKs) are a family of Ca^{2+}/calmodulin (CaM)-dependent protein kinases involved in the regulation of microvascular permeability. The function of MLCK is to phosphorylate the

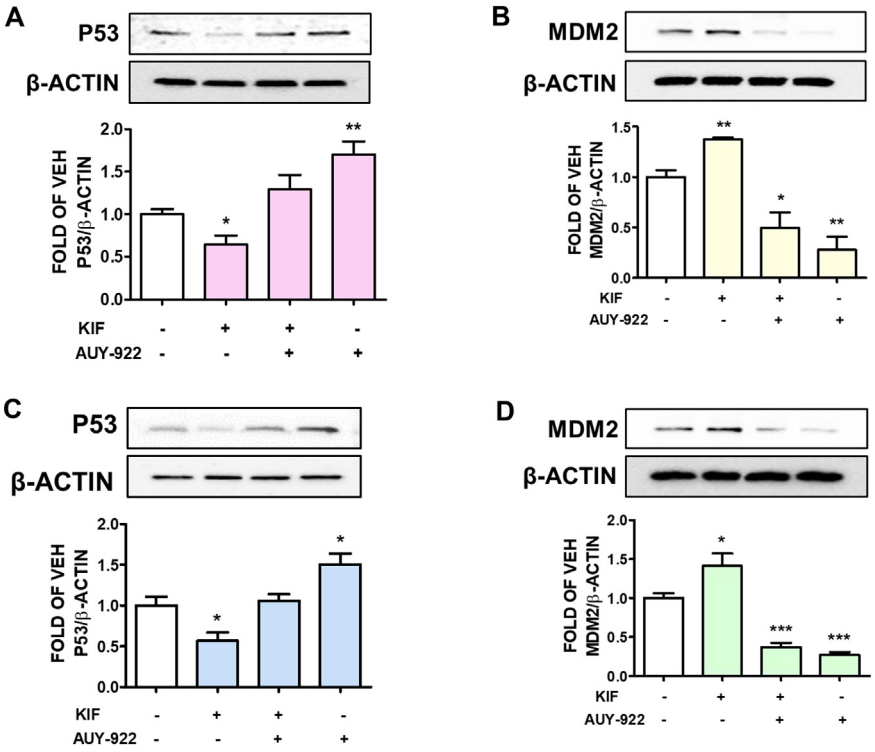

Fig. 2. Effects of KIF and AUY-922 on P53 regulation. Western Bot analysis of (A) P53 and β-actin, (B) MDM2 and β-actin expression after 24 h treatment of BPAEC with either KIF (5 μM) or vehicle (0.1% DMSO); and post-treatment with AUY-922 (2 μM) or vehicle (0.1% DMSO) for 16 h. The blots shown are representative of 3 independent experiments. The signal intensity of P53 and MDM2 was analyzed by densitometry, and the protein levels were normalized to β-actin. $^{*}P < 0.05$, $^{**}P < 0.01$ vs vehicle. Means ± SEM. Western Bot analysis of (C) P53 and β-actin, (D) MDM2 and β-actin expression after 24 h treatment of HuLEC-5a with either KIF (5 μM) or vehicle (0.1% DMSO) and post-treatment with AUY-922 (2 μM) or vehicle (0.1% DMSO) for 16 h. The blots shown are representative of 3 independent experiments. Signal intensity of P53 and MDM2 was analyzed by densitometry. Protein levels were normalized to β-actin. $^{*}P < 0.05$, *** < 0.001 vs vehicle. Means ± SEM.

regulatory MLC2, which produces F-actin. The posttranslational modification of MLC is a fundamental molecular cascade towards the regulation of lung endothelial barrier integrity (Rigor et al., 2013). The pMLC2 triggers the ATP-dependent actomyosin contraction to potentiate endothelial cell membrane retraction, intercellular gap formation, and vascular barrier disruption (Shen et al., 2010).

Luminespib deactivates Cofilin, which is a small (19-kDa) ubiquitous actin-binding protein associated with the regulation of cell protrusions (Uddin et al., 2019b). Phosphorylated cofilin does not bind to the actin, thus Cofilin is deactivated by phosphorylation to support lung endothelial barrier integrity. Plasma membrane phosphatidylinositol-4,5-bisphosphate (PIP_2) is also associated with the cortical actin formation by inhibiting Cofilin (Belvitch et al., 2018). In intestinal epithelial cells, hypoxia initiates the activation of Cofilin, which in turn increases endothelial permeability, as reflected in the decreased TEER measurements. Those values reflect changes in endothelial and epithelial permeability (Song et al., 2019). Similar reductions have been observed in models of ALI, indicating the disruption of tight junction proteins (Birukova et al., 2015; Kovacs-Kasa et al., 2018).

KIF has been shown to activate Cofilin by dephosphorylation (Akhter et al., 2020b). In the present study the Hsp90 inhibitor AUY-922 counteracted those events. It was also demonstrated that a mild UPR induction due to Hsp90 inhibition induces key players in the mediation of the UPR signaling, including the BiP, endoplasmic reticulum oxidoreductin-1 alpha (ERO1-Lα), and protein disulfide isomerase (PDI) (Barabutis, 2019a). The importance of UPR in mediating normal respiratory functions is underlined by the fact that knock-in mice expressing a mutant BiP protein suffered from respiratory dysfunction due to abnormal secretion of lung surfactant by the alveolar type II epithelial cells (Kubra et al., 2020b; Barabutis, 2020c).

UPR is also essential for ER homeostasis during growth (Kubra et al., 2020b; Barabutis, 2020c). IRE1α increased the level of tumor necrosis factor alpha (TNF-α) in the porcine reproductive and respiratory syndrome, while PERK exerted the opposite effects (Chen et al., 2018). In another study, PERK knock-out (KO) mice were used to examine the effects of transverse aortic constriction (TAC)-induced lung fibrosis and lung vascular remodeling. Chronic TAC initiated the apoptosis of cardiomyocytes and exacerbated lung remodeling in the mutant mice. UPR affects P53 expression levels, since UPR induction elevates P53 levels, while UPR suppressors reduce them (Akhter et al., 2019).

P53 is a transcription factor essential for the regulation of vascular integrity, and involved in the lung function. Moreover, it exerts its anti-inflammatory effects by suppressing nuclear factor-kappa B (NF-κB) (Uddin and Barabutis, 2020). Mycoplasma infection activates NF-κB via P53 suppression, thus contributing to the development of tumors (Gudkov and Komarova, 2016). Moreover, P53 suppresses NF-κB by repressing the glucocorticoid receptor (Murphy et al., 2011). It was also shown that the induction of P53 protects against the lipopolysaccharides (LPS)-triggered endothelial barrier dysfunction (Barabutis, 2020b). In another study, the expression levels of major pro-inflammatory mediators were more prominent in P53 KO mice than the wild type counteracts due to LPS treatment (Liu et al., 2009; Uddin et al., 2020b). LPS was shown to downregulate P53 expression via the induction of MDM2. Indeed, P53 mediates the protective effects of Hsp90 inhibition by modulating the RhoA/MLC2 pathway (Barabutis, 2020d), thus reducing the formation of the F-actin fibers (Barabutis et al., 2015). In the present effort, we show that Hsp90 inhibition by AUY-922 counteracts the Kifunensine-induced P53 suppression by suppressing MDM2.

Our study demonstrates for the first time that the deteriorating effects of the UPR suppressor Kifunensine in lung endothelial cells are counteracted by the UPR inducer AUY-922. Thus, we suggest that UPR manipulation may serve as a promising therapeutic strategy towards lung disease, including the COVID-19 related ARDS. Future studies will follow to investigate the exact UPR branches involved in those phenomena, by employing

advanced models of genetically modified mice. Those mutants will not express the inositol-requiring enzyme-1α (IRE1α), or the protein kinase R (PKR)-like endoplasmic reticulum kinase (PERK) and activating transcription factor 6α (ATF6α).

Funding

Our research is supported by the 1) R&D, Research Competitiveness Subprogram (RCS) of the Louisiana Board of Regents through the Board of Regents Support Fund (LEQSF(2019-22)-RD-A-26) (PI: NB) 2) Faculty Research Support Program from Dean's Office, College of Pharmacy, ULM (PI: NB) and 3) NIGMS/NIH (5 P20GM103424-15, 3 P20 GM103424-15S1)

Declaration of competing interest

No conflicts of interest, financial or otherwise, are declared by the authors.

References

Abbasi, M., Amanlou, M., Aghaei, M., Bakherad, M., Doosti, R., Sadeghi-Aliabadi, H., 2020. New heat shock protein (Hsp90) inhibitors, designed by pharmacophore modeling and virtual screening: synthesis, biological evaluation and molecular dynamics studies. J. Biomol. Struct. Dyn. 38 (12), 3462–3473.

Akhter, M.S., Uddin, M.A., Barabutis, N., 2019. Unfolded protein response regulates P53 expression in the pulmonary endothelium. J. Biochem. Mol. Toxicol. 33 (10), e22380.

Akhter, M.S., Uddin, M.A., Barabutis, N., 2020a. P53 Regulates the Redox Status of Lung Endothelial Cells. Inflammation 43 (2), 686–691.

Akhter, M.S., Kubra, K.T., Uddin, M.A., Barabutis, N., 2020b. Kifunensine compromises lung endothelial barrier function. Microvasc. Res. 132, 104051.

Barabutis, N., 2019a. Unfolded Protein Response in Acute Respiratory Distress Syndrome. Lung 197 (6), 827–828.

Barabutis, N., 2019b. Unfolded Protein Response supports endothelial barrier function. Biochimie 165, 206–209.

Barabutis, N., 2020a. Heat shock protein 90 inhibition in the inflamed lungs. Cell Stress Chaperones 25 (2), 195–197.

Barabutis, N., 2020b. P53 in lung vascular barrier dysfunction. Vasc Biol 2 (1), E1–E2.

Barabutis, N., 2020c. Unfolded protein response in lung health and disease. Front Med 7.

Barabutis, N., 2020d. P53 in acute respiratory distress syndrome. Cell. Mol. Life Sci., 1–3 https://doi.org/10.1007/s00018-020-03629-1.

Barabutis, N., Siejka, A., 2020. The highly interrelated GHRH, p53, and Hsp90 universe. Cell Biol. Int. 44 (8), 1558–1563.

Barabutis, N., Handa, V., Dimitropoulou, C., Rafikov, R., Snead, C., Kumar, S., et al., 2013. LPS induces pp60c-src-mediated tyrosine phosphorylation of Hsp90 in lung vascular endothelial cells and mouse lung. Am. J. Phys. Lung Cell. Mol. Phys. 304 (12), L883–L893.

Barabutis, N., Dimitropoulou, C., Birmpas, C., Joshi, A., Thangjam, G., Catravas, J.D., 2015. p53 protects against LPS-induced lung endothelial barrier dysfunction. Am. J. Phys. Lung Cell. Mol. Phys. 308 (8), L776–L787.

Barabutis, N., Schally, A.V., Siejka, A., 2018a. P53, GHRH, inflammation and cancer. EBioMedicine 37, 557–562.

Barabutis, N., Dimitropoulou, C., Gregory, B., Catravas, J.D., 2018b. Wild-type p53 enhances endothelial barrier function by mediating RAC1 signalling and RhoA inhibition. J. Cell. Mol. Med. 22 (3), 1792–1804.

Barabutis, N., Uddin, M.A., Catravas, J.D., 2019. Hsp90 inhibitors suppress P53 phosphorylation in LPS - induced endothelial inflammation. Cytokine 113, 427–432.

Belvitch, P., Htwe, Y.M., Brown, M.E., Dudek, S., 2018. Cortical Actin Dynamics in Endothelial Permeability. Curr. Top. Membr. 82, 141–195.

Birukova, A.A., Meng, F., Tian, Y., Meliton, A., Sarich, N., Quilliam, L.A., et al., 2015. Prostacyclin post-treatment improves LPS-induced acute lung injury and endothelial barrier recovery via Rap1. Biochim. Biophys. Acta 1852 (5), 778–791.

Chen, W.Y., Schniztlein, W.M., Calzada-Nova, G., Zuckermann, F.A., 2018. Genotype 2 Strains of Porcine Reproductive and Respiratory Syndrome Virus Dysregulate Alveolar Macrophage Cytokine Production via the Unfolded Protein Response. J. Virol. 92 (2).

Felip, E., Barlesi, F., Besse, B., Chu, Q., Gandhi, L., Kim, S.W., et al., 2018. Phase 2 Study of the HSP-90 Inhibitor AUY922 in Previously Treated and Molecularly Defined Patients with Advanced Non-Small Cell Lung Cancer. J. Thorac. Oncol. 13 (4), 576–584.

Good, R.J., Hernandez-Lagunas, L., Allawzi, A., Maltzahn, J.K., Vohwinkel, C.U., Upadhyay, A.K., et al., 2018. MicroRNA dysregulation in lung injury: the role of the miR-26a/EphA2 axis in regulation of endothelial permeability. Am. J. Phys. Lung Cell. Mol. Phys. 315 (4), L584–L594.

Gudkov, A.V., Komarova, E.A., 2016. p53 and the Carcinogenicity of Chronic Inflammation. Cold Spring Harb. Perspect. Med. 6 (11).

Joshi, A.D., Dimitropoulou, C., Thangjam, G., Snead, C., Feldman, S., Barabutis, N., et al., 2014. Heat shock protein 90 inhibitors prevent LPS-induced endothelial barrier dysfunction by disrupting RhoA signaling. Am. J. Respir. Cell Mol. Biol. 50 (1), 170–179.

Kovacs-Kasa, A., Kim, K.M., Cherian-Shaw, M., Black, S.M., Fulton, D.J., Verin, A.D., 2018. Extracellular adenosine-induced Rac1 activation in pulmonary endothelium: Molecular mechanisms and barrier-protective role. J. Cell. Physiol. 233 (8), 5736–5746.

Kubra, K.T., Akhter, M.S., Uddin, M.A., Barabutis, N., 2020a. P53 versus inflammation: an update. Cell Cycle 19 (2), 160–162.

Kubra, K.T., Akhter, M.S., Uddin, M.A., Barabutis, N., 2020b. Unfolded protein response in cardiovascular disease. Cell. Signal. 73, 109699.

Kubra, K.T., Uddin, M.A., Akhter, M.S., Barabutis, N., 2020c. Hsp90 inhibitors induce the unfolded protein response in bovine and mice lung cells. Cell. Signal. 67, 109500.

Liu, G., Park, Y.J., Tsuruta, Y., Lorne, E., Abraham, E., 2009. p53 Attenuates lipopolysaccharide-induced NF-kappaB activation and acute lung injury. J. Immunol. 182 (8), 5063–5071.

Muller, L., Schaupp, A., Walerych, D., Wegele, H., Buchner, J., 2004. Hsp90 regulates the activity of wild type p53 under physiological and elevated temperatures. J. Biol. Chem. 279 (47), 48846–48854.

Murphy, S.H., Suzuki, K., Downes, M., Welch, G.L., De Jesus, P., Miraglia, L.J., et al., 2011. Tumor suppressor protein (p)53, is a regulator of NF-kappaB repression by the glucocorticoid receptor. Proc. Natl. Acad. Sci. U. S. A. 108 (41), 17117–17122.

Rigor, R.R., Shen, Q., Pivetti, C.D., Wu, M.H., Yuan, S.Y., 2013. Myosin light chain kinase signaling in endothelial barrier dysfunction. Med. Res. Rev. 33 (5), 911–933.

Scieglinska, D., Krawczyk, Z., Sojka, D.R., Gogler-Piglowska, A., 2019. Heat shock proteins in the physiology and pathophysiology of epidermal keratinocytes. Cell Stress Chaperones 24 (6), 1027–1044.

Shen, Q., Rigor, R.R., Pivetti, C.D., Wu, M.H., Yuan, S.Y., 2010. Myosin light chain kinase in microvascular endothelial barrier function. Cardiovasc. Res. 87 (2), 272–280.

Solopov, P., Biancatelli, R., Marinova, M., Dimitropoulou, C., Catravas, J.D., 2020. The HSP90 Inhibitor, AUY-922, Ameliorates the Development of Nitrogen Mustard-Induced Pulmonary Fibrosis and Lung Dysfunction in Mice. Int. J. Mol. Sci. 21 (13).

Song, H., Zhang, J., He, W., Wang, P., Wang, F., 2019. Activation of Cofilin Increases Intestinal Permeability via Depolymerization of F-Actin During Hypoxia in vitro. Front. Physiol. 10, 1455.

Torres Acosta, M.A., Singer, B.D., 2020. Pathogenesis of COVID-19-induced ARDS: implications for an ageing population. Eur. Respir. J. 56 (3), 2002049.

Uddin, M.A., Barabutis, N., 2020. P53 in the impaired lungs. DNA Repair (Amst) 95, 102952.

Uddin, M.A., Akhter, M.S., Siejka, A., Catravas, J.D., Barabutis, N., 2019a. P53 supports endothelial barrier function via APE1/Ref1 suppression. Immunobiology 224 (4), 532–538.

Uddin, M.A., Akhter, M.S., Singh, S.S., Kubra, K.T., Schally, A.V., Jois, S., et al., 2019b. GHRH antagonists support lung endothelial barrier function. Tissue Barriers 7 (4), 1669989.

Uddin, M.A., Kubra, K.T., Sonju, J.J., Akhter, M.S., Seetharama, J., Barabutis, N., 2020a. Effects of Heat Shock Protein 90 Inhibition In the Lungs. Med. Drug Discov. 6.

Uddin, M.A., Akhter, M.S., Kubra, K.T., Barabutis, N., 2020b. P53 deficiency potentiates LPS-Induced acute lung injury in vivo. Curr. Res. Physiol. 3, 30–33.